Regenerative Therapy 26 (2024) 932–940

Contents lists available at ScienceDirect

Regenerative Therapy

journal homepage: http://www.elsevier.com/locate/reth

Original Article

Exosomes derived from epidermal growth factor-like domain protein 6-preconditioned mesenchymal stem cells for diabetic wound healing

Chen Gong [a], Chengde Xia [b], Linbo Liu [a, *]

[a] Department of Plastic Surgery, The First Affiliated Hospital of Zhengzhou University, Zhengzhou, Henan, China
[b] Department of Burn Surgery, The First People's Hospital of Zhengzhou, Zhengzhou, Henan, China

ARTICLE INFO

Article history:
Received 7 August 2024
Received in revised form
30 August 2024
Accepted 23 September 2024

Keywords:
Diabetic wound healing
Mesenchymal stem cells
Epidermal growth factor-like domain protein 6
Exosomes
Hydrogel

ABSTRACT

Diabetic wounds are difficult to repair effectively in the clinic. Tissue engineering based on mesenchymal stem cells (MSCs) showed great therapeutic potential in wound healing. MSCs-derived exosome could reproduce the effect of MSCs by transferring the bioactive substance to the recipient cells. The biological function of exosomes was determined by the state of the derived MSCs. In this study, we cultured hUC-MSCs with EGFL6 and isolated EGFL6-preconditioned exosomes (EGF-Exos), and then investigated the effect of EGF-Exos on wound healing. The results revealed that EGF-Exos promoted the proliferation and migration of HUVECs, had the anti-inflammtory function and improved angiogenesis. Moreover, we fabricated Gelama hydrogel to load EGF-Exos to repair diabetic wounds. *In vivo* results showed that EGF-Exos contributed to the repair of diabetic wound and provided valuable data for understanding the role of EGF-Exos in diabetic wound healing.

1. Introduction

Diabetes is a common metabolic disease with a high risk of severe disability. 15% of diabetics may suffer from foot ulcers, causing high medical costs and poor quality of life [1,2]. Wound healing is a complicated and well-orchestrated biological process such as damaged vascular network, acute inflammation and impaired extracellular matrix (ECM) deposition [3–5]. Current treatment strategies for healing chronic wounds should focus on the phases including inhibiting inflammation, promoting angiogenesis and preventing infection [6–8].

Mesenchymal stem cells (MSCs)-based tissue engineering showed great therapeutic potential in wound healing [9–11]. Recent study has shown that MSCs possess great anti-inflammatory effect [12]. Human umbilical cord MSCs (hUC-MSCs) exhibit favorable biological properties including an abundant tissue source, large expansion capacity and a painless collection process [13]. Exosomes, small extracellular vesicles, ranged in size from 30 to 150 nm, are rich in proteins, mRNAs and miRNAs [14,15]. Previous studies have shown that MSCs-derived exosome could replicated the effect of MSCs by transferring the bioactive substance to the recipient cells [16,17]. In particular, the biological function of exosomes was determined by the state of the derived MSCs. For example, exosome derived from kartogenin-preconditioned MSCs can promote chondrogenesis [18].

The ability of proliferation and migration of endothelial cells play important role in angiogenesis. Previous studies reported that the epidermal growth factor-like domain protein 6 (EGFL6) is essential for the regulation of angiogenesis [19]. EGFL6 is a member of the EGF superfamily of proteins. Previous studies showed that EGFL6 secreted by osteoblast-like cells regulated the migration and angiogenesis of endothelial cell via the ERK signaling pathway [20]. However, the effect of exosomes derived from EGFL6-preconditioned hUC-MSCs (EGF-Exos) on wound healing is still unknown.

Hydrogel is the desirable tissue engineering material to encapsulate exosomes to enhance vascularization or facilitate tissue regeneration. In this study, we prepared Gelma hydrogel to entrap EGF-Exos. Furthermore, we evaluated the feasibility of applying EGF-Exos as a new biomimetic tool to achieve chronic wound healing. Our findings could lead to new the novel therapeutic strategies for chronic skin wounds.

2. Material and methods

2.1. hUCMSCs characterization

hUCMSCs were incubated in chondrogenic differentiation medium (Cyagen, China), adipogenic (Cyagen, China), osteogenic

* Corresponding author.
E-mail address: linboliu1@163.com (L. Liu).
Peer review under responsibility of the Japanese Society for Regenerative Medicine.

https://doi.org/10.1016/j.reth.2024.09.009

(Cyagen, China) for 21 days, 21 days and 14 days respectively. Then, the differentiated MSCs were fixed by 4% paraformaldehyde (PFA) and stained by Alcian Blue, Oil O Red and Alizarin Red respectively.

2.2. Isolation and identification of EGF-Exos

Recombinant EGFL6 protein was purchased from R&D Systems. hUCMSCs were cultured in the Ultra culture medium (Lonza, USA, 12–725F) contained with 10% exosome-free FBS and 200 ng/mL EGFL6 protein. EGF-Exos were extracted from conditional medium according to the previous methods [21] by gradient ultracentrifugation. In brief, the condition medium was centrifuged at 2000×*g* for 10 min and then 10,000×*g* for 30 min (4 °C) to remove dead cells and cell debris respectively. Subsequently, the medium was centrifuged at 100,000×*g* for 90 min (4 °C), washed with PBS, and centrifuged at 100,000×*g* for 90 min (4 °C) again to isolate the Exos.

The size distribution and concentration of sEVs were analyzed by Nanosight NS300 system (Malvern, UK). The morphology of sEVs was identified by Transmission electron microscopy (TEM). The marker proteins of sEVs were identified through western blotting.

2.3. PKH-26 staining

Fluorescent labeling of EGF-Exos was carried out according to the manufacturer's protocols. Briefly, PKH-26 solution (Sigma, USA, SLB6089) was incubated with exosomes in PBS. Excessive dye from labeled exosomes was removed by ultracentrifugation at 100,000×*g* for 1 h at 4 °C. Exosome pellets stained by PKH-26 were resuspended with 200 μl cold PBS. The labeled exosomes were co-cultured with HUVECs for 24 h, and then the cells were washed with PBS and fixed in 4% paraformaldehyde. The uptake of PKH-26-labeled EGF-Exos by HUVECs was then observed by fluorescent microscopy.

2.4. Cell proliferation assay

HUVECs were cultured in endothelial cell medium supplemented with 5% fetal bovine serum, 1% endothelial cell growth supplement (ECGS) and 1% penicillin-streptomycin (Sciencell, Carlsbad, CA, USA). HUVECs were co-incubated with EGF-Exos for 24h and 48h in 96-well plates. Cell counting kit-8 (CCK8) were purchased from Kumamoto (Japan). 10 μl CCK-8 was added into the medium. After being co-cultured for 3h, the proliferation ability of HUVECs was measured by 450 nm absorbance values using an enzyme linked immunosorbent assay plate reader.

2.5. Western blot assay

Western blotting was carried out to assess the expressions of proteins. Protein lysates were obtained from human umbilical vein endothelial cells and EGF-Exos using RIPA lysis buffer. The protein concentrations determination was performed using a BCA Protein Assay Reagent Kit (Thermo, USA). Equivalent amounts of proteins (20000 μg) were separated on 10% sodium dodecyl sulfate-polyacrylamide gel electrophoresis (SDS-PAGE) and then transferred to 0.22 μm polyvinylidene fluoride (PVDF) membrane. After being blocked by 5% non-fat dry milk, the membranes were incubated with primary antibodies overnight at 4 °C. After incubation with horseradish peroxidase (HRP)-conjugated species-matched secondary antibodies for 1h at room temperature. ImmunoStar Western C (LI-COR, USA) was used to observe the proteins band. Primary antibody included anti-CD63(Abcam, USA), anti-CD81(Abcam, USA), CD9(Abcam, USA), anti-β-actin (CST, USA,3700, 1:1000).

2.6. Real-time quantitative polymerase chain reaction (qPCR) assay

Total RNA isolation from HUVECs was performed using TRIzol reagent (Invitrogen, Carlsbad, CA, USA) according to the manufacturer's instructions. RNA quality and quantity determination were carried out using nanodrop (Thermo Scientific). RNA (1000 ng) was reverse-transcribed into cDNA using the revert first strand cDNA synthesis kit (Yesen, China). 20 μl reaction volumes (10 μl SYBR, 0.8 μl primers, 2 μl cDNA, 7.2 μl H_2O) was completed and then qPCR was performed. The primer sequence of above gene was listed in Table 1.

2.7. Immunofluorescence staining

HUVECs were cultured in the medium contained EGF-Exos, following TNF-α (10 ng/mL) stimulation for 24 h. Then, the cells were fixed using 4% PFA for 10 min and next washed by PBS for three times. Then, HUVECs were treated with 0.25% Triton X-100 and then blocked with 5% donkey serum. HUVECs were incubated with primary anti-body VEGF (Abcam, USA) overnight at 4 °C. After being washed by PBS, HUVECs were incubated with the secondary antibody (Invitrogen, USA) and cultured with DAPI for 10 min in dark environment. Finally, HUVECs were visualized under the confocal microscope (Carl Zeiss, Germany). The excitation wavelength of DAPI was 405 nm and that of VEGF was 488 nm.

2.8. Wound healing assay

The effect of EGF-Exos on HUVECs migration was evaluated by “wound healing” assay. Briefly, a sterile pipette was used to created “wound” after HUVECs growing in full density in 24 well plates. Then, cell debris were removed by PBS. HUVECs were incubated in the fresh medium contained EGF-Exos for 8 h. Subsequently, the medium was removed and then the cells were fixed by PFA for 15min. The cells were stained with 0.2% crystal violet hydrate solution and then observed using microscope.

2.9. Swelling ratio and degradation behaviors assay

Gelma hydrogel was purchased from Engineering for life company. The samples were incubated with PBS for 24 h [22]. After removing the surface water, the swelling samples were weighted at different time points. The formula below was used to calculate the swelling ratios of the hydrogels:

$$\text{Swelling ratio} = \frac{W_t - W_d}{W_d} \times 100\%$$

W_d was the dry weight of the hydrogel, and W_t was the swollen weight of the hydrogel.

Table 1
The primer sequence of inflammatory genes.

Gene	Sequences
IL-6	F-5'-GGCCAGAACTTCCCAACCA-3'
	R-5'-ACCCTCCATAATGTCATACCC-3'
TNF-α	F-5'-CAGGCGGTGCCTATGTCTC-3'
	R-5'- CGATCACCCCGAAGTTCAGTAG-3'
IL-10	F-5'- CTCCAAGCCAAAGTCCTTAGAG-3'
	R-5'- TGTAGACCATGTAGTTGAGGTCA-3'
GAPDH	F-5'-AGGTCGGTGTGAACGGATTTG-3'
	F-5'-TGTAGACCATGTAGTTGAGGTCA-3'

The specimen were soaked in PBS at 37 °C to evaluate the degradation behaviors of hydrogels. At given time points, the surface supernatant was removed and then the weight of hydrogels was weighted. The following formula was used to calculate the degradation ratios of hydrogels:

$$\text{Degradation ratio} = \frac{W_t}{W_0} \times 100\%$$

where W_0 was the initial weight of the sample, and W_t was the weight of the sample at a specific time point.

2.10. Animal experiments

All surgical procedures required the agreement of the ethical review committee of The First Affiliated Hospital of Zhengzhou University. Diabetic mice model was fabricated as previously described [2]. Briefly, female C57BL/6 mice were divided into four groups. The mice were anaesthetized by injecting avertin and then the dorsal hair of diabetic mice was shaved. A standardized full thickness wound (8 mm diameters) was built. Gelma hydrogel loading EGF-Exos was implanted into the wound. To avoid antibacterial interference, mouse was caged individually in Specific

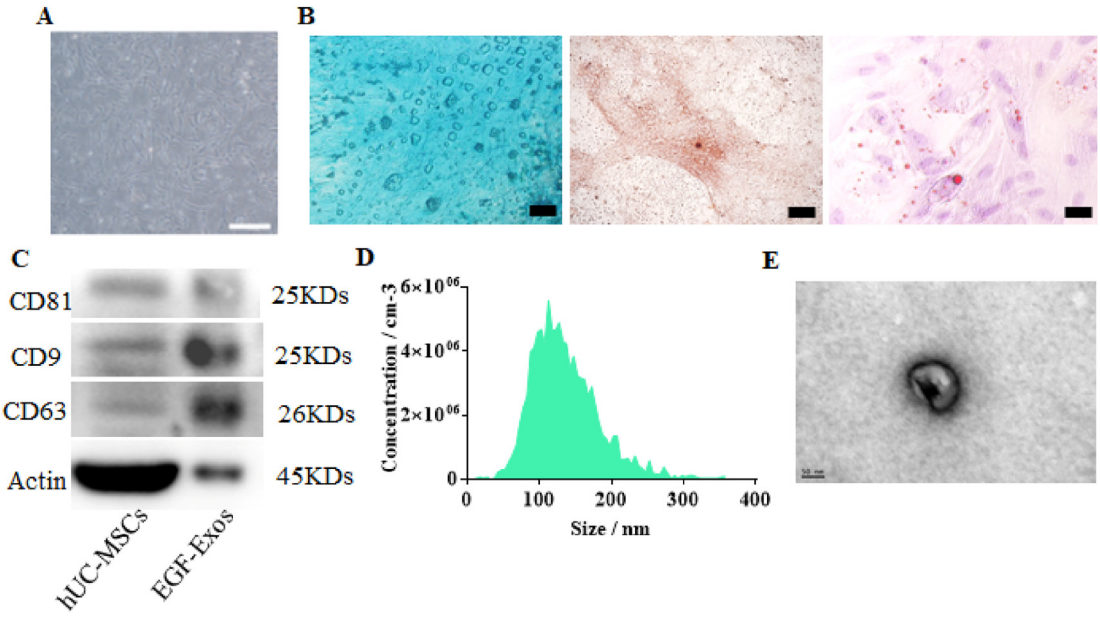

Fig. 1. Identification of hUC-MSCs and EGF-Exos. (A) hUC-MSCs represented spindle-like morphology. Scale bar: 150 μm. (B) hUC-MSCs showed muti-lineage differentiation of chondrogenesis, osteogenesis and adipogenesis. Scale bar: 100 μm. (C) The surface marker of EGF-Exos including CD81, CD9, CD63 were characterized by Western blot. (D) Particle size distribution of EGF-Exos was measured by nanoparticle tracking analysis. (E) The morphology of EGF-Exos was visualized by TEM. Scale bar: 50 nm.

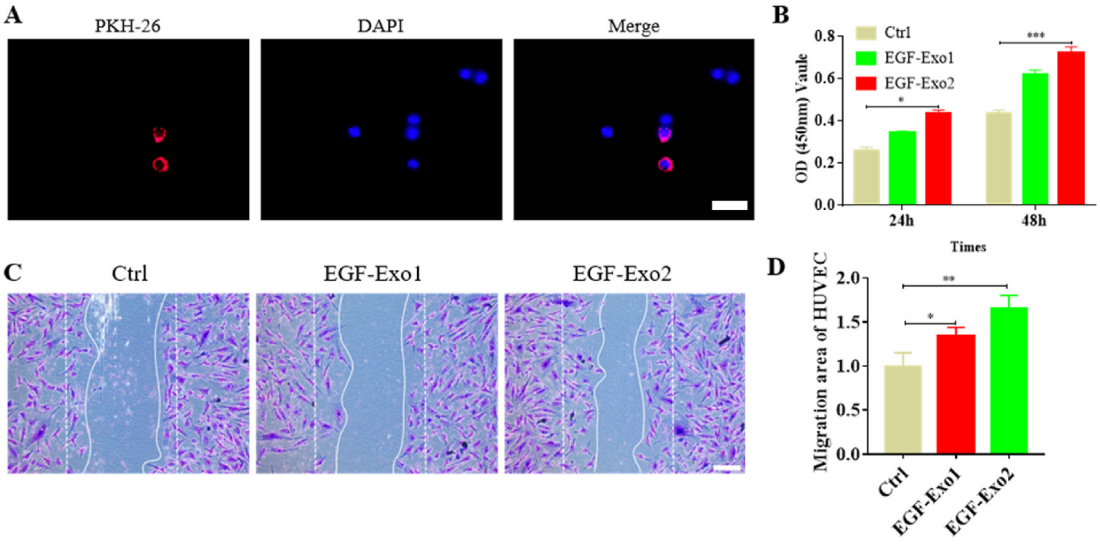

Fig. 2. EGF-Exos promote the proliferation, migration of HUVECs. (A) Representative image of PKH-26 labeled EGF-Exos. HUVECs were cultured with the PKH-26 labeled for 24 h. Scale bar:20 μm. (B) CCK-8 assay of HUVECs incubated with EFG-Exos for 24 h and 48 h. Ctrl group means that HUVECs cultured in medium contained TNF-α (10 ng/mL). EGF-Exos1 group means that HUVECs cultured in medium with exosomes (10 μg/mL), following TNF-α (10 ng/mL) stimulation. EGF-Exos2 group means that HUVECs cultured in medium with exosomes (20 μg/mL), following TNF-α (10 ng/mL) stimulation. *P < 0.05, ***P < 0.001. (C) Photographs of "wound healing" assay of HUVECs after 8 h incubated with EGF-Exos and (D) Quantitative analysis of the relative migrated percentage of HUVECs in different groups.

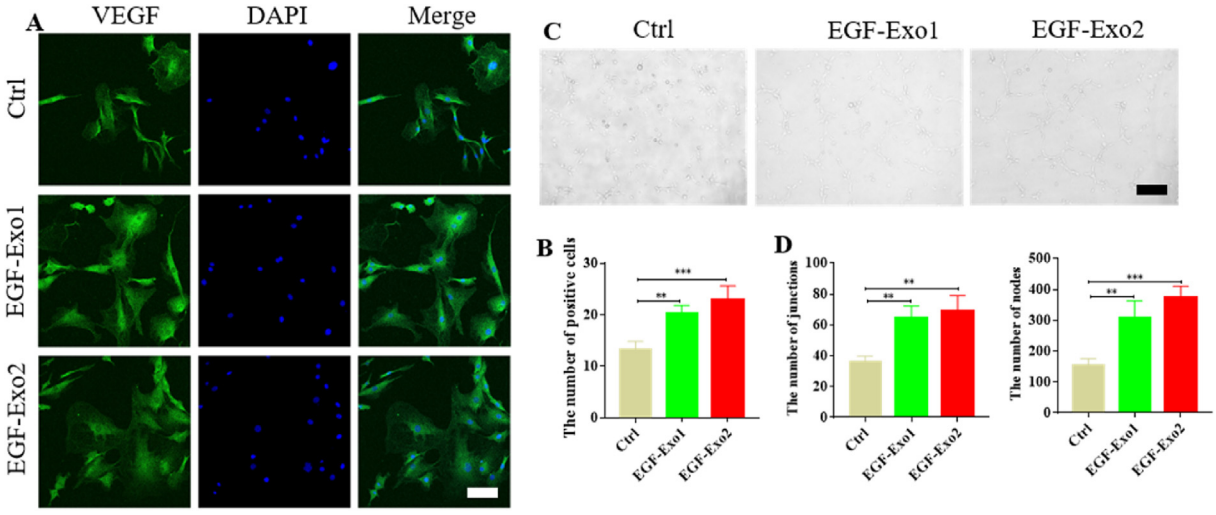

Fig. 3. EGF-Exos promote angiogenesis of HUVECs *in vitro*. (A) Immunofluorescence of vascular endothelial growth factor (VEGF) visualized using confocal fluorescence microscope. Scale bar:50 μm. (B) The number of VEGF positive cells. **P < 0.01, ***P < 0.001. (C) Matrigel-based assay for HUVECs cultured with EGF-Exos. Scale bar:100 μm. (D) The number of junction and nodes about tube formation assay were analyzed by Image J. **P < 0.01, ***P < 0.001.

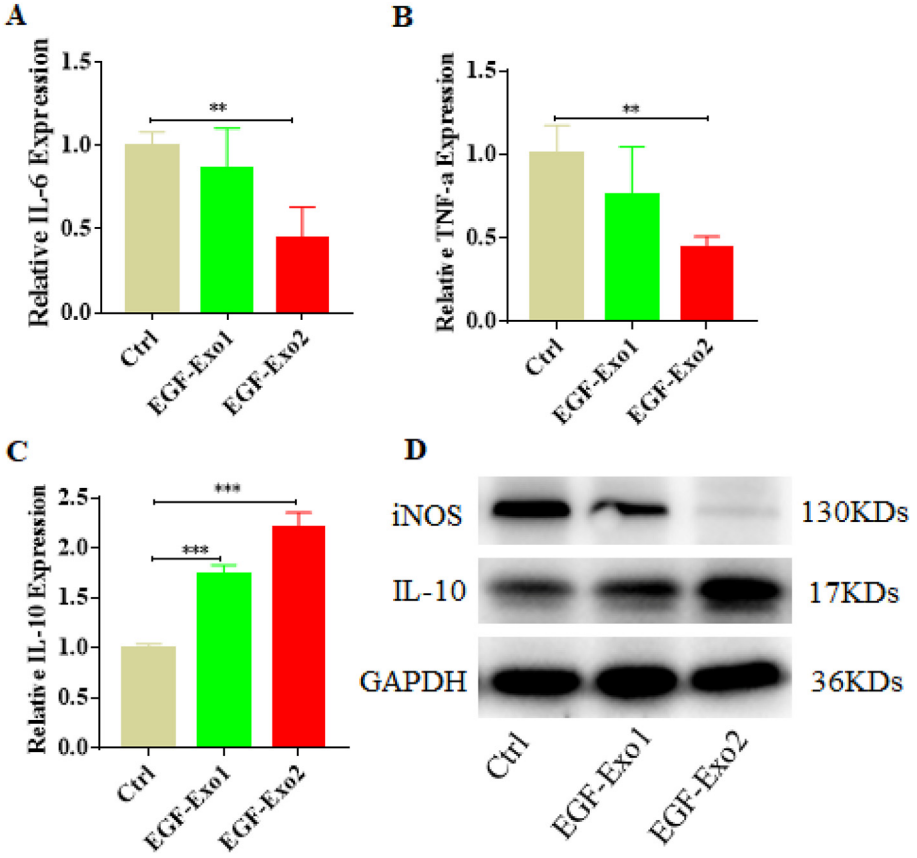

Fig. 4. EGF-Exos have anti-inflammatory effect *in vitro*. (A) The inflammatory gene including IL-6, (B) TNF-α measured by qPCR. **P < 0.01. (C) The anti-inflammatory gene IL-10 was estimated via qPCR. ***P < 0.001. (D) The proteins of iNOS and IL-10 were evaluated using Western blot. Ctrl group means that HUVECs were cultured in the medium contained TNF-α (10 ng/mL) for 24 h. EGF-Exo group means that HUVECs were cultured in the medium contained EGF-Exo, following TNF-α (10 ng/mL) stimulation for 24 h.

Pathogen Free (SPF) environmental conditions. The recovery of diabetic wound was evaluated by digital image which was taken at 0, 1, 3, 5, 7, 9, 11 and 13 days. The following formula was used to calculate the wound size:

Percent wound size reduction (%) = $(A_0\text{-}A_t)/A_0 \times 100\%$

A_0 means the initial wound area (t = 0). A_t means the wound area at a time interval (t ≥ 1).

The animals were sacrificed at 7,11,15 days after surgery, and the skin tissue around the wound was collected to measure the formation of novel vessel generated in the wound.

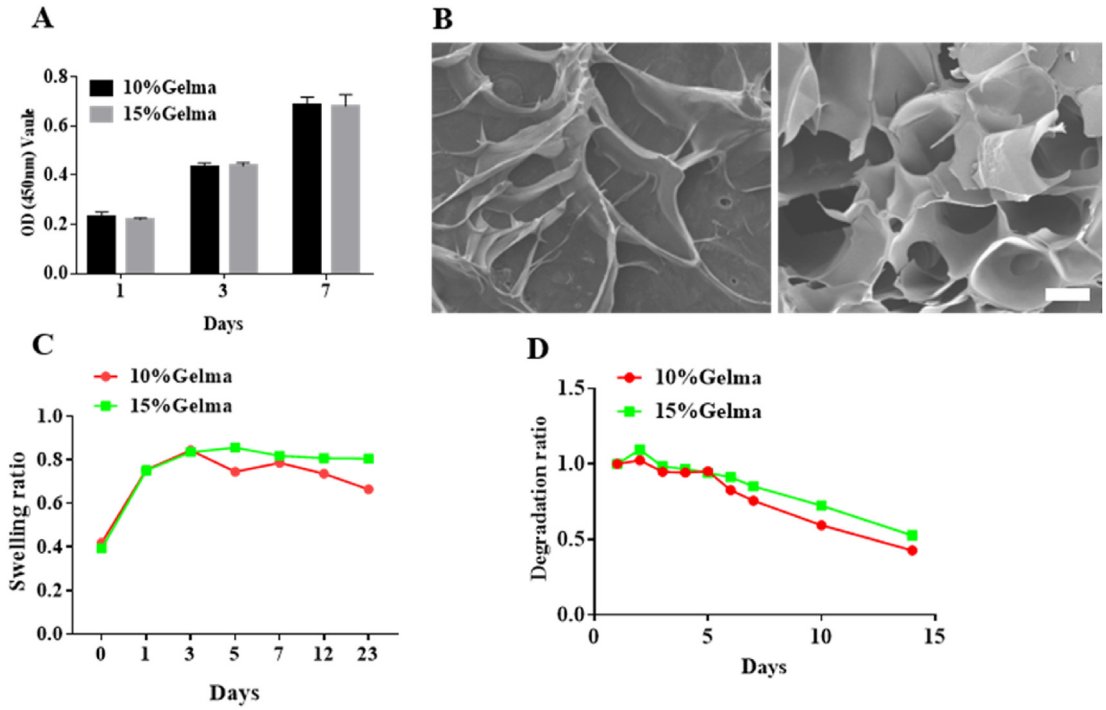

Fig. 5. Characterization of Gelma hydrogel. (A) Cell viability of HUVECs cultured with Gelma. (B) Scanning electron micrographs of Gelma. Scale bars: 200 μm. (C) Swelling ratio of the hydrogels in PBS (pH 7.2) at 37 °C. (D) Degradation ratio of Gelma hydrogel.

2.11. Histology and immunohistochemical analysis

The skin tissue samples were fixed in 4% paraformaldehyde for 24 h and then dehydrate in a gradient alcohol. After being embedded in paraffin, the specimens were sliced in 5 μm thickness. The skin tissue sections were evaluated by masson trichrome and immunohistochemical staining.

Immunohistochemical staining was performed according to the previous protocol [23]. Briefly, sodium citrate solution was used to treat the skin tissue sections to epitope retrieval. Then, the samples were treated with a primary antibody like CD31(Abcam, USA) overnight at 4 °C. Subsequently, the samples were incubated with a second antibody and then stained with hematoxylin. The sections were clearly observed under the microscope.

2.12. Statistical analysis

The results are presented as mean ± standard deviation (SD). For comparison of two groups, the unpaired Student's t test was used. One-way analysis of variance (ANOVA) was used for the comparison of multiples groups. Differences were considered statistically significant when $P < 0.05$.

3. Results

3.1. Identification of hUC-MSCs and EGF-Exos

The density of hUC-MSCs cultured in 6 cm dish reached 60% confluence, hUC-MSCs represented spindle-like morphology visualized by microscope (Fig. 1A). When hUC-MSCs were cultured in adipogenesis, osteogenesis and chondrogenesis induced medium, hUC-MSCs were induced to adipogenic, osteogenic and chondrogenic cells respectively (Fig. 1B). EGF-Exos were isolated by gradient ultracentrifugation and characterized by different experiments. The extracellular vesicles-related specific marker including CD63, CD81, CD9 were positively expressed on EGF-Exos (Fig. 1C). The image of TEM revealed that the morphology of EGF-Exos showed typical sphere-shaped bilayer membrane structure. Moreover, the data of nanoparticle tracking analysis showed that the diameter of exosomes was about 127 nm, and the concentration of EGF-Exos was 2×10^{11} particles/mL (Fig. 1D).

3.2. EGF-Exos promote the proliferation, migration of HUVECs

To observed whether EGF-Exos were uptaken by HUVECs, the exosomes were stained with PKH-26 and the stained EGF-Exos were incubated with HUVECs for 24h. As showed in Fig. 2A, the PKH-26 labeled EGF-Exos which showed red fluorescence were internalized by HUVECs and distributed around the nuclei which was stained in blue fluorescence by DAPI. In addition, we evaluated the viability of HUVECs cultured with EGF-Exos using CCK-8 experiment (Fig. 2B). The results showed that the number of HUVECs was significantly increased after EGF-Exos treatment for 24 and 48h, indicating that EGF-Exos2 has significant effect on the cell viability in HUVECs. Subsequently, to estimate the effect of EGF-Exos on cell migration, we treated HUVECs with EGF-Exos for 8h. The results revealed that compared to the control group, the migration area of HUVECs treated with EGF-Exos2 was significantly increased (Fig. 2C, D).

3.3. EGF-Exos promote angiogenesis of HUVECs in vitro

To further observe the effect of EGF-Exos on the angiogenesis *in vitro*, VEGF immunofluorescence was carried out. Green fluorescent cells were more abundant in the EGF-Exos group, compared to the control group, indicating EGF-Exos enhanced the expression of VEGF in HUVECs and could promoted angiogenesis *in vitro* (Fig. 3 A, B). Subsequently, matrigel-based assay was used to assess the effect of EGF-Exos on the endothelial network formation ability of HUVECs. The results showed that the endothelial network formation ability of HUVECs was increased by EGF-Exos, compared the control group. The number of nodes and junction about matrigel-

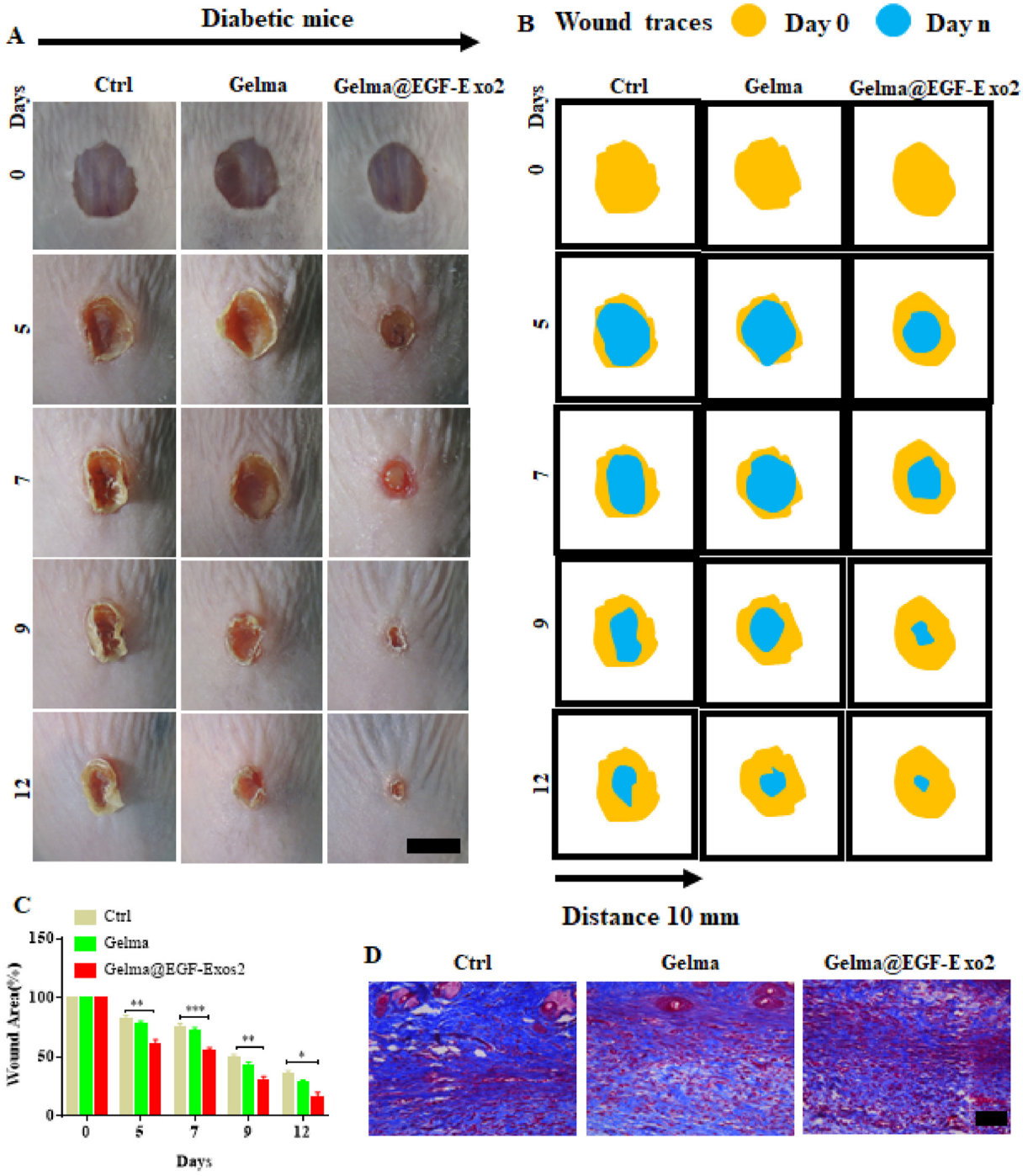

Fig. 6. The effect of 15%Gelma hydrogel loading EGF-Exos2 on the diabetic wound healing. (A) Gross macroscopic of the size change of the excision wounds made in dorsal skin of diabetic mice with different time periods. (B) Traces of wound bed closure for each treatment group *in vivo*. Light brown area indicated the wounds area at 0 day and the blue area indicated the wounds area at n (n = 5, 7, 9 and 12) days. (C) The statistical analysis of wound area was conducted to show the healing efficiency among the groups. *P < 0.05, **P < 0.01, ***P < 0.001. (D) Masson's trichrome staining images of wound beds at 12 days. Blue areas represented the newly deposited collagen fibers in the wound beds. Scale bars: 200 μm.

based assay showed that EGF-Exos treatment significantly increased the endothelial network formation ability of HUVECs.

3.3.1. *EGF-Exos have anti-inflammatory effect in vitro*

HUVECs were stimulated with TNF-α (10 ng/mL) and EGF-Exos for 24h. Then the inflammatory gene IL-6 and TNF-α were measured to observe the anti-inflammatory effect *in vitro*. The results exhibited that EGF-Exos1 group show the similar gene expression level of IL-6 and TNF-α with control group, while the level of IL-6 and TNF-α genes was significantly increased in EGF-Exos2 group (Fig. 4 A, B). Moreover, EGF-Exos treatment obviously enhanced the expression of IL-10, compared to the control group (Fig. 4C). Consistently, compared to the control and EGF-Exos1 group, the protein of iNOS was downregulated in EGF-Exos2 group, while the anti-inflammatory protein IL-10 was upregulated in EGF-Exos2 group (Fig. 4 D). In general, the above results

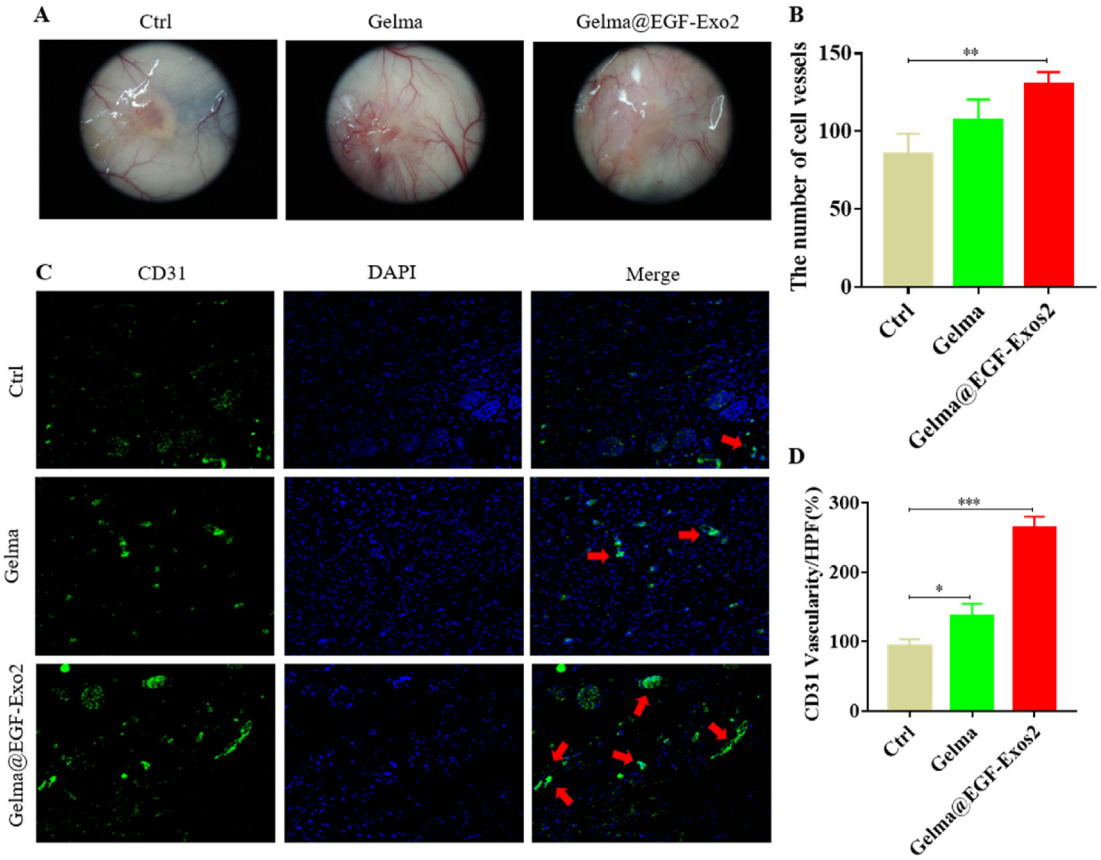

Fig. 7. Gelma@EGF-Exos2 promote angiogenesis *in vivo*. (A) Representative images of vessel formation at the wound beds at 12 days. (B) The quantitative analysis of vessel formation in the diabetic wound beds. **P < 0.01. (C) CD31 immunofluorescent staining of the diabetic wound beds and (D) the quantitative of the expression of CD31 in the diabetic wound beds. *P < 0.05, ***P < 0.001.

demonstrated that EGF-Exos exhibited powerful anti-inflammatory effect *in vitro*.

3.4. Characterization of Gelma hydrogel

To observe the cytotoxicity of Gelma hydrogel, HUVECs were cultured with hydrogel. As illustrated in Fig. 5 A, OD values were increased during the process of incubation, indicating that the number of HUVECs was increased and the hydrogel possess desirable biocompatibility. The reticular porous structure of the hydrogels was observed using SEM (Fig. 5 B). The diameter of 15% Gelma hydrogel was smaller than 10% Gelma hydrogel. The swelling behavior of the hydrogels was revealed in Fig. 5C. The results showed that the swelling ratio of the hydrogels was gradually increased during the first 3 days. 15% Gelma hydrogel had the higher swelling ratio than 10% Gelma hydrogel. Moreover, the Gelma hydrogel showed good degradation ratio which decreased 50% in the incubation of 15 days ((Fig. 5 D).

3.5. The effect of 15%Gelma hydrogel loading EGF-Exos2 on the diabetic wound healing

We fabricated 15% Gelma loading the EGF-Exos2 (20 μg/mL) for the treatment of the diabetic wound. Gross macroscopic evaluation of the wound was performed at 0,5,7,9 and 12 days. As showed in Fig. 6 A and B, the wound regions of the diabetic mice were gradually decreased in all groups, while compared to the 85% wound area of control group and 77.7% wound area of Gelma group at 5 days, the wound area of Gelma@EGF-Exos2 group was significantly decreased. Moreover, the wound area size was reduced 83.7% at 12 days, which was significantly higher than other two groups whose wound area sizes were decreased 65.4% and 72.3% respectively at 12 days (Fig. 6C). Moreover, the collagen fibers in Gelma@EGF-Exos2 group were more extensive and orderly-arranged than that other two groups (Fig. 6 D).

3.6. Gelma@EGF-Exos2 promote angiogenesis in vivo

Representative photograph of the angiogenesis in diabetic wound beds showed that the number of novel generated vessel around the center of wound in Gelma@EGF-Exos2 group was obviously increased compared to the other two group at 12 days (Fig. 7 A, B). Moreover, there were more intensive newly formatted vessels observed in Gelma@EGF-Exos2 group. CD31 immunohistochemical staining was performed to further investigate the angiogenesis effect of Gelma@EGF-Exos2 *in vivo* (Fig. 7C). As a specific marker of vein endothelial cells, CD31 was selected to label the newly formed blood vessels, the number and area of CD31 positive vascular on Gelma@EGF-Exos2 group was significantly increased compared to other two groups (Fig. 7 D), indicating that Gelma@EGF-Exos2 therapy contributed to the regeneration of blood vessels *in vivo* and enhance the blood supply for wound, improving the healing ratio of diabetic wound.

4. Discussion

The skin wound caused by diabetes is difficult to repair effectively in the clinic [24,25]. Currently, MSC-based therapy shows

desirable potential for healing diabetic wound [26–29]. Herein, we treated hUC-MSCs with EGFL6 and isolated exosomes derived from EGFL6-preconditional hUC-MSCs (EGF-Exos). We found that EGF-Exos promoted the proliferation and migration of HUVECs. Moreover, EGF-Exos possessed anti-inflammatory effects and improved angiogenesis. In addition, we fabricated Gelma hydrogel to loading EGF-Exos to implanted into the wound region. *In vivo* results revealed that Gelma@ EGF-Exos effectively promoted diabetic wound healing.

hUC-MSCs are a desirable cell source for the reasons that hUC-MSCs are accessible, have ideal proliferation capability and facilitate acquisition process [18,30]. hUC-MSCs preconditioned with EGFL6 are essential for improving angiogenesis. Previous studies showed that the desirable function of MSC-based therapies was mainly attributed to paracrine, as exosomes can create an optimal microenvironment for maintaining dynamic cellular homeostasis [27,31]. However, the effect of EGF-Exos on diabetic wounds is still unknown.

Wounds repair and regeneration are the complicated process, involving hemostasis, inflammation, hyperplasia and remodeling [32,33]. Hyperglycemia caused by diabetic wounds worsened inflammation and vascular lesions, delaying the process of wound healing. Previous study showed that increased proinflammatory cellular infiltrates composed largely of neutrophils and macrophages contribute to delayed healing of chronic ulcers [34,35]. Herein, we found that EGF-Exos could be internalized by HUVECs and achieved the effects of anti-inflammatory by decreasing the expression levels of TNFα and IL-1β. It has been shown that IL-1β and TNFα derived from proinflammatory cells elevated metalloproteinases and degraded the local ECM, resulting in the destruction of cell migration [36]. Subsequently, we investigated the function of EGF-Exos on the proliferation and migration of HUVECs. The results showed that EGF-Exos significantly promoted the proliferation and migration of HUVECs, indicating that EGF-Exos contributed to the growth of HUVECs toward the wound regions. Abundant nutrient exchange and adequate oxygen supply transported by vascular network have been shown to have a positive effect on cell migration and distribution [37]. The newly generated vascular network is important for the process of wound healing [38–40]. In this study, we found that EGF-Exos contributes to the regeneration of blood vessels *in vivo* and improves the blood supply to the wound, thereby improving the healing ratio of diabetic wound. Moreover, EGF-Exos enhanced the formation of collagen which was main component of skin main component of skin.

In general, this study demonstrated that EGF-Exos contributed to the repair of diabetic wounds by effectively promoting the proliferation and migration of HUVECs, exhibiting the anti-inflammatory function and improving angiogenesis.

Declaration of competing interest

The authors reported no potential conflict of interest.

Acknowledgement

The authors declare that they have no conflict of interest.

References

[1] Yan C, Chen J, Wang C, Yuan M, Kang Y, Wu Z, et al. Milk exosomes-mediated miR-31-5p delivery accelerates diabetic wound healing through promoting angiogenesis. Drug Deliv 2022;29(1):214–28.
[2] Lv F, Wang J, Xu P, Han Y, Ma H, Xu H, et al. A conducive bioceramic/polymer composite biomaterial for diabetic wound healing. Acta Biomater 2017;60:128–43.
[3] Bodnar RJ. Chemokine regulation of angiogenesis during wound healing. Adv Wound Care 2015;4(11):641–50.
[4] Schultz GS, Wysocki A. Interactions between extracellular matrix and growth factors in wound healing. Wound Repair Regen 2009;17(2):153–62.
[5] Wang C, Wang M, Xu T, Zhang X, Lin C, Gao W, et al. Engineering bioactive self-healing antibacterial exosomes hydrogel for promoting chronic diabetic wound healing and complete skin regeneration. Theranostics 2019;9(1):65–76.
[6] Chen T, Chen Y, Rehman HU, Chen Z, Yang Z, Wang M, et al. Self-healing, and tissue-adhesive hydrogel for wound dressing. ACS Appl Mater Interfaces 2018;10(39):33523–31.
[7] Wang H, Xu Z, Zhao M, Liu G, Wu J. Advances of hydrogel dressings in diabetic wounds. Biomater Sci 2021;9(5):1530–46.
[8] Duan S, Wang F, Cao J, Wang C. Exosomes derived from MicroRNA-146a-5p-enriched bone marrow mesenchymal stem cells alleviate intracerebral hemorrhage by inhibiting neuronal apoptosis and microglial M1 polarization. Drug Des Devel Ther 2020;14:3143–58.
[9] Nan W, Xu Z, Chen Z, Yuan X, Lin J, Feng H, et al. Bone marrow mesenchymal stem cells accelerate the hyperglycemic refractory wound healing by inhibiting an excessive inflammatory response. Mol Med Rep 2017;15(5):3239–44.
[10] Liu Y, Chen J, Liang H, Cai Y, Li X, Yan L, et al. Human umbilical cord-derived mesenchymal stem cells not only ameliorate blood glucose but also protect vascular endothelium from diabetic damage through a paracrine mechanism mediated by MAPK/ERK signaling. Stem Cell Res Ther 2022;13(1):258.
[11] Zhang B, Wang M, Gong A, Zhang X, Wu X, Zhu Y, et al. HucMSC-exosome mediated-wnt 4 signaling is required for cutaneous wound healing. Stem Cell 2015;33(7):2158–68.
[12] Feng Y, Wu JJ, Sun ZL, Liu SY, Zou ML, Yuan ZD, et al. Targeted apoptosis of myofibroblasts by elesclomol inhibits hypertrophic scar formation. EBioMedicine 2020;54:102715.
[13] Hu H, Dong L, Bu Z, Shen Y, Luo J, Zhang H, et al. miR-23a-3p-abundant small extracellular vesicles released from Gelma/nanoclay hydrogel for cartilage regeneration. J Extracell Vesicles 2020;9(1):1778883.
[14] Yu B, Zhang X, Li X. Exosomes derived from mesenchymal stem cells. Int J Mol Sci 2014;15(3):4142–57.
[15] Yu X, Odenthal M, Fries JW. Exosomes as miRNA carriers: formation-function-future. Int J Mol Sci 2016;17(12).
[16] Mathieu M, Martin-Jaular L, Lavieu G, Thery C. Specificities of secretion and uptake of exosomes and other extracellular vesicles for cell-to-cell communication. Nat Cell Biol 2019;21(1):9–17.
[17] Sadeghipour S, Mathias RA. Herpesviruses hijack host exosomes for viral pathogenesis. Semin Cell Dev Biol 2017;67:91–100.
[18] Jing H, Zhang X, Luo K, Luo Q, Yin M, Wang W, et al. miR-381-abundant small extracellular vesicles derived from kartogenin-preconditioned mesenchymal stem cells promote chondrogenesis of MSCs by targeting TAOK1. Biomaterials 2020;231:119682.
[19] Mas VR, Maluf DG, Archer KJ, Yanek KC, Fisher RA. Angiogenesis soluble factors as hepatocellular carcinoma noninvasive markers for monitoring hepatitis C virus cirrhotic patients awaiting liver transplantation. Transplantation 2007;84(10):1262–71.
[20] Chim SM, Qin A, Tickner J, Pavlos N, Davey T, Wang H, et al. EGFL6 promotes endothelial cell migration and angiogenesis through the activation of extracellular signal-regulated kinase. J Biol Chem 2011;286(25):22035–46.
[21] Thery C, Amigorena S, Raposo G, Clayton A. Isolation and characterization of exosomes from cell culture supernatants and biological fluids. Curr Protoc Cell Biol 2006;3(3 22).
[22] Park H, Guo X, Temenoff JS, Tabata Y, Caplan AI, Kasper FK, et al. Effect of swelling ratio of injectable hydrogel composites on chondrogenic differentiation of encapsulated rabbit marrow mesenchymal stem cells in vitro. Biomacromolecules 2009;10(3):541–6.
[23] Chen Y, Wu T, Huang S, Suen CW, Cheng X, Li J, et al. Sustained release SDF-1alpha/TGF-beta1-loaded silk fibroin-porous gelatin scaffold promotes cartilage repair. ACS Appl Mater Interfaces 2019;11(16):14608–18.
[24] Dash BC, Xu Z, Lin L, Koo A, Ndon S, Berthiaume F, et al. Stem cells and engineered scaffolds for regenerative wound healing. Bioengineering (Basel) 2018;5(1).
[25] Gkikas M, Avery RK, Olsen BD. Thermoresponsive and mechanical properties of Poly(L-proline) gels. Biomacromolecules 2016;17(2):399–406.
[26] Walter MN, Wright KT, Fuller HR, MacNeil S, Johnson WE. Mesenchymal stem cell-conditioned medium accelerates skin wound healing: an in vitro study of fibroblast and keratinocyte scratch assays. Exp Cell Res 2010;316(7):1271–81.
[27] Safari S, Malekvandfard F, Babashah S, Alizadehasl A, Sadeghizadeh M, Motavaf M. Mesenchymal stem cell-derived exosomes: a novel potential therapeutic avenue for cardiac regeneration. Cell Mol Biol (Noisy-le-grand) 2016;62(7):66–73.
[28] Rani S, Ryan AE, Griffin MD, Ritter T. Mesenchymal stem cell-derived extracellular vesicles: toward cell-free therapeutic applications. Mol Ther 2015;23(5):812–23.
[29] Smith AN, Willis E, Chan VT, Muffley LA, Isik FF, Gibran NS, et al. Mesenchymal stem cells induce dermal fibroblast responses to injury. Exp Cell Res 2010;316(1):48–54.
[30] Bello AB, Kim Y, Park S, Muttigi MS, Kim J, Park H, et al. Matrilin3/TGFbeta3 gelatin microparticles promote chondrogenesis, prevent hypertrophy, and induce paracrine release in MSC spheroid for disc regeneration. NPJ Regen Med 2021;6(1):50.

[31] Ti D, Hao H, Fu X, Han W. Mesenchymal stem cells-derived exosomal microRNAs contribute to wound inflammation. Sci China Life Sci 2016;59(12):1305–12.
[32] Gurtner GC, Werner S, Barrandon Y, Longaker MT. Wound repair and regeneration. Nature 2008;453(7193):314–21.
[33] Liu W, Yu M, Xie D, Wang L, Ye C, Zhu Q, et al. Melatonin-stimulated MSC-derived exosomes improve diabetic wound healing through regulating macrophage M1 and M2 polarization by targeting the PTEN/AKT pathway. Stem Cell Res Ther 2020;11(1):259.
[34] Sindrilaru A, Peters T, Wieschalka S, Baican C, Baican A, Peter H, et al. An unrestrained proinflammatory M1 macrophage population induced by iron impairs wound healing in humans and mice. J Clin Invest 2011;121(3):985–97.
[35] Eming SA, Martin P, Tomic-Canic M. Wound repair and regeneration: mechanisms, signaling, and translation. Sci Transl Med 2014;6(265):265sr266.
[36] Tarnuzzer RW, Schultz GS. Biochemical analysis of acute and chronic wound environments. Wound Repair Regen 1996;4(3):321–5.
[37] Han X, Sun M, Chen B, Saiding Q, Zhang J, Song H, et al. Lotus seedpod-inspired internal vascularized 3D printed scaffold for bone tissue repair. Bioact Mater 2021;6(6):1639–52.
[38] Shi M, Gao Y, Lee L, Song T, Zhou J, Yan L, et al. Adaptive gelatin microspheres enhanced stem cell delivery and integration with diabetic wounds to activate skin tissue regeneration. Front Bioeng Biotechnol 2022;10:813805.
[39] Braddock M, Campbell CJ, Zuder D. Current therapies for wound healing: electrical stimulation, biological therapeutics, and the potential for gene therapy. Int J Dermatol 1999;38(11):808–17.
[40] Phinney DG. Functional heterogeneity of mesenchymal stem cells: implications for cell therapy. J Cell Biochem 2012;113(9):2806–12.